What we know and what we don't know about the proton spin after 30 years

Xiangdong Ji[1,2]✉, *Feng Yuan*[3]✉ *and Yong Zhao*[4]✉

Abstract | More than three decades ago, the European Muon Collaboration published a surprising result on the spin structure of the proton: the spins of its three quark components account for only a small part of the spin of the proton. Ever since, theoretical and experimental progress has been made in understanding the origins of the proton spin. In this Review, we discuss what has been learned so far, what is still missing and what could be learned from the upcoming experiments, including the Jefferson Lab 12 GeV upgrade and the proposed Electron-Ion Collider. In particular, we focus on first-principles calculations and experimental measurements of the total gluon helicity ΔG, and the quark and gluon orbital angular momenta.

The proton is a spin-1/2 particle, thought to be fundamental when discovered in 1917 by Ernest Rutherford[1]. However, the subsequent measurement of its magnetic moment[2] showed a significant deviation from the value expected for a point-like object[3]. The proton substructure, along with the origin of its spin and magnetic moment, has intrigued nuclear and particle physicists ever since.

Every model of the proton ought to give an explanation for its spin: from the Skyrme model[4], to Gell–Mann and Zweig's quark model[5,6], and to many other models proposed in the 1970s and 1980s (REFS[7,8]). The simplest and most successful one has been the quark model, which inspired, among other things, the discovery of quantum chromodynamics (QCD)[9] — the fundamental theory of strong interactions. The non-relativistic quark model has an exceedingly simple explanation for the proton/neutron spin and the associated magnetic moments[10], as well as their excitations[11]. The three constituent quarks are all in the *s*-wave orbit, and their spins couple to 1/2 in a way that is consistent with the $SU(2)_{spin} \times SU(3)_{flavour}$ combined spin–flavour symmetry[12].

The quark model picture was directly tested through measurements of the polarized deep inelastic scattering of leptons (electrons or muons) off a polarized proton target[13]. In 1987, the European Muon Collaboration (EMC) reported that the fraction of the proton spin carried by the spins of three quarks at the measured scale Q^2 is[14,15]

$$\Delta\Sigma(Q^2 = 10.7\ \mathrm{GeV}^2) = 0.060 \pm 0.047 \pm 0.069, \qquad (1)$$

which is practically nothing. The EMC data also showed a significant deviation from the Ellis–Jaffe sum rule for the polarized structure function based on the quark picture[16]. The EMC result shocked the physics community, and created the so-called proton spin 'crisis' or proton spin problem. The discrepancy has since inspired a large number of experimental and theoretical studies, which have been reviewed in a number of papers[17–22]. The most important lesson learned so far is that the underlying theory for the proton structure, QCD, has a much more sophisticated way to build up the proton spin.

QCD is fundamental and beautiful on the one hand, and sophisticated and defying simple ways to understand it on the other. For example, in a QCD framework, it is no longer feasible, or we have failed so far, to come up with an entire quark and gluon wave function for the proton and to check the content of its various components. Therefore, we will consider instead the so-called sum rules or decompositions of the spin into various physical parts. This has been the main approach to understand the origins of the proton spin so far.

This is not a comprehensive review of hadron spin physics. Nor is it meant to be an update on other reviews[19,22], which have done an excellent job. Rather, this Review focuses on the questions related to the origins of the proton spin. We mainly discuss issues such as: does it make sense to talk about different parts of the proton spin? What will be an interesting and physically meaningful decomposition for the spin? To what extent do we believe that we can measure each part experimentally? How can one calculate these parts in fundamental theory and put the results to experimental tests? We hope that, after more than 30 years after the EMC result, this Review can help the broader physics

[1]*Center for Nuclear Femtography, SURA, Washington DC, USA.*

[2]*Department of Physics, University of Maryland, College Park, MD, USA.*

[3]*Nuclear Science Division, Lawrence Berkeley National Laboratory, Berkeley, CA, USA.*

[4]*Physics Department, Brookhaven National Laboratory, Upton, NY, USA.*

✉*e-mail: xji@umd.edu; fyuan@lbl.gov; yzhao@bnl.gov*

https://doi.org/10.1038/s42254-020-00248-4

Key points

- There are two established approaches to look at the composition of the proton spin: the frame-independent spin structure (or the Ji sum rule) and the infinite-momentum-frame or parton spin structure (or the Jaffe–Manohar sum rule).
- In the frame-independent approach, the quark orbital and gluon angular momentum contributions can be extracted from the moments of the generalized parton distributions. Results from the Jefferson Lab 6 GeV and HERMES experiments suggest that there is a substantial quark orbital contribution.
- In terms of partons, the quark and gluon helicity contributions have a simple physical interpretation, and the result from Relativistic Heavy Ion Collider spin experiments has provided a first important constraint on the total gluon helicity.
- The development of a large-momentum effective theory along with lattice quantum chromodynamics simulations provide first-principles calculations of the spin structure. The results on the quark and gluon helicity contributions, and the quark orbital and gluon angular momentum contributions have provided the first complete theoretical picture.
- The Jefferson Lab 12 GeV programme will provide better information on the quark orbital angular momentum and gluon angular momentum. The future Electron-Ion Collider will provide high-precision measurements on the gluon helicity and gluon angular momentum.

community to understand what we know now, what we don't and what we can expect in the future. In particular, how will the Electron-Ion Collider (EIC) help to answer the fundamental questions about the origins of the proton spin[23,24].

Spin structure in sum rules

Without knowing the wave function of the composite system, the angular momentum (AM), or spin structure, can be studied through the various contributions to the total. Thus, to explore origins of the proton spin, one can start from the QCD AM operator $\mathbf{J}_{\mathrm{QCD}}$ in terms of individual sources $\mathbf{J}_\alpha$,

$$\mathbf{J}_{\mathrm{QCD}} = \sum_\alpha \mathbf{J}_\alpha, \tag{2}$$

through which, the spin projection $\hbar/2$ can be expressed as a sum of different contributions.

This approach has some limitations. Since the proton is an eigenstate of the relativistic Pauli–Lubanski spin[25], the individual contributions can only be the quantum mechanical expectation values of the AM sources from the entire bound-state wave function. Moreover, they are 'renormalization-scale dependent', because individual operators are not separately conserved, and the resulting ultraviolet divergences must be renormalized meaning that the short-distance physics is included in the effective AM operators[26]. In non-relativistic systems, with the exception of particles moving in a magnetic field, the AM sources corresponding to different physical degrees of freedom obey the separate AM commutation relations. In quantum field theories, the simple commutation relations at the bare-field level are violated when dressed with interactions, and only the total AM commutation relations are protected by the rotational symmetry[27]. Finally, gauge symmetry imposes important constraints on what is physically measurable.

Still, there exists more than one way to split the AM operator and derive spin sum rules for the proton. A physically interesting spin sum rule should have the following properties:

- Experimental measurability. The interest in the proton spin began with the EMC data. Many of the follow-up experiments, including HERMES and COMPASS, the polarized Relativistic Heavy Ion Collider (RHIC)[28], the Jefferson Lab (JLab) 12 GeV upgrade[29] and the EIC[23,24], have been partially motivated to search for a full understanding of the proton spin.
- Frame independence. As spin is an intrinsic property of a particle, it is natural to look for a description of its structure independent of its momentum. To know how the individual contributions to the total spin depend on the reference frame requires an understanding of the properties of the Lorentz transformations of $\mathbf{J}_\alpha$. As the proton structure probed in high-energy scattering is best described in the infinite-momentum frame (IMF), a partonic picture of the spin is interesting in this special frame of reference.
- According to the above remarks, two sum rules have been well established in the literature (TABLE 1): the frame-independent one[30] and the IMF one[31], as we explain below.

QCD sources of angular momentum. To obtain a spin sum rule, an expression for the QCD AM operator is needed. This can be derived through Noether's theorem[32] based on the space-time symmetry of the QCD Lagrangian density

$$\mathcal{L}_{\mathrm{QCD}} = -\frac{1}{4}F_a^{\mu\nu}F_{\mu\nu a} + \sum_f \bar{\psi}_f(i\not{D} - m_f)\psi_f, \tag{3}$$

where $F_a^{\mu\nu}$ (μ and $\nu = 0, 1, 2, 3$ are Lorentz indices) is a gluon field strength tensor or simply gluon field with colour indices $a = 1, \ldots, 8$ and ψ_f is a quark spinor field of flavour $f = u, d, s, \ldots$ (up, down, strange, ...), and m_f is the quark mass. The relation between the gauge field and gauge potential A_a^μ is $F_a^{\mu\nu} = \partial^\mu A^\nu - \partial^\nu A_a^\mu - g_s f^{abc} A_b^\mu A_c^\nu$ with g_s as the strong coupling constant. The covariant derivative is $D^\mu = \partial^\mu + ig_s A^\mu$ and $\not{D} = D^\mu \gamma_\mu$ with γ^μ as Dirac matrices. $A^\mu = A_a^\mu t^a$ and t^a are the generators of the SU(3) colour group and f^{abc} is the structure constant. A straightforward calculation yields the canonical AM expression[31]

$$\mathbf{J}_{\mathrm{QCD}} = \int \mathrm{d}^3\mathbf{x}\left[\psi_f^\dagger \frac{\boldsymbol{\Sigma}}{2}\psi_f + \psi_f^\dagger \mathbf{x}\times(-i\nabla)\psi_f + \mathbf{E}_a \times \mathbf{A}_a + E_a^i(\mathbf{x}\times\nabla)A_a^i\right], \tag{4}$$

where $\boldsymbol{\Sigma} = \mathrm{diag}(\sigma, \sigma)$ with σ being the Pauli matrix, and the contraction of flavour (f) and colour (a) indices, as well as the spatial Lorentz index i, is implied. E_a^i ($\mathbf{E}_a$) is the colour electric fields F^{i0}. The above expression contains four different terms, each of which has clear physical meaning in free-field theory. The first term corresponds to the quark spin, the second to the quark orbital AM (OAM), the third to the gluon spin and the last one to the gluon OAM. Apart from the first term, the rest are not

Pauli–Lubanski spin
A spin four-vector operator generalized for relativistic particles.

Partonic picture
The distribution of physical observables in partons with different momentum fractions x.

Table 1 | **Two established proton spin sum rules, frame independent and infinite-momentum frame**

Spin sum rule	Formula	Terms	Characteristics
Frame independent (Ji)[30]	$\frac{1}{2}\Delta\Sigma + L_q^z + J_g = \frac{\hbar}{2}$	$\Delta\Sigma/2$ is the quark helicity L_q^z is the quark OAM J_g is the gluon contribution	The quark and gluon contributions, J_q and J_g, can be obtained from the GPD moments. A similar sum rule also works for the transverse angular momentum and has a simple parton interpretation
Infinite-momentum frame (Jaffe–Manohar)[31]	$\frac{1}{2}\Delta\Sigma + \Delta G + \ell_q + \ell_g = \frac{\hbar}{2}$	ΔG is the gluon helicity ℓ_q and ℓ_g are the quark and gluon canonical OAM, respectively	All terms have partonic interpretations; ℓ_q and ℓ_g are twist-three quantities. ΔG is measurable in experiments, including the RHIC spin and the EIC; ℓ_q and ℓ_g can be extracted from twist-three GPDs

EIC, Electron-Ion Collider; GPD, generalized parton distribution; OAM, orbital angular momentum; RHIC, Relativistic Heavy Ion Collider.

gauge invariant under the general gauge transformation, $\psi \to U(x)\psi$ and $A^\mu \to U(x)(A^\mu + (i/g_s)\partial^\mu)U^\dagger(x)$, where $U(x)$ is an SU(3) matrix. However, the total is invariant under the gauge transformation up to a surface term at infinity, which can be ignored in physical matrix elements.

Theoretically, the canonical form of the AM operator allows the derivation of an infinite number of spin sum rules with different choices of gauges and/or frames of reference (hadron momentum)[20,33]. In practice, only the IMF, relevant for interpreting high-energy scattering experiments, and a physical gauge, such as the Coulomb gauge, have shown to be related to experimental observables.

Using the Belinfante improvement procedure[34], one can obtain a gauge-invariant form from equation 4 (REF.[30])

$$\mathbf{J}_{\mathrm{QCD}} = \int \mathrm{d}^3x \left[\psi_f^\dagger \frac{\boldsymbol{\Sigma}}{2} \psi_f + \psi_f^\dagger \mathbf{x} \times (-i\boldsymbol{\nabla} - g_s \mathbf{A})\psi_f + \mathbf{x} \times (\mathbf{E} \times \mathbf{B}) \right], \tag{5}$$

where **B** is the colour magnetic fields. All three terms are gauge invariant, with the second term being the mechanical or kinetic OAM and the third term the gluon AM.

To evaluate the quark orbital and gluon contributions in a polarized proton state, we need the matrix elements of the QCD energy-momentum tensor (EMT), which can be split into the sum of the quark and gluon contributions, $T^{\mu\nu} = T_q^{\mu\nu} + T_g^{\mu\nu}$, following the Belinfante improvement. The EMT defines the momentum density, which is the source of the AM density. The non-diagonal matrix elements among states with different momenta and spins have been parameterized as[30]

$$\langle P'S'|T_{q/g}^{\mu\nu}|PS\rangle = \overline{U}(P'S')\left[A_{q/g}(\Delta^2)\gamma^{(\mu}\overline{P}^{\nu)} + B_{q/g}(\Delta^2)\frac{\overline{P}^{(\mu}i\sigma^{\nu)\alpha}\Delta_\alpha}{2M} + \ldots \right] U(PS), \tag{6}$$

where P, M, S represent the nucleon momentum, mass and polarization, respectively, $\overline{P}^\mu = (P^\mu + P'^\mu)/2$ is an average momentum, $\Delta^\mu = P'^\mu - P^\mu$ is the difference. U and $\overline{U}$ are Dirac spinors for the nucleon state, and A and B are the scalar form factors depending on the momentum transfer squared, Δ^2.

Helicity sum rules. Without loss of generality, one can assume the proton three-component momentum to be $\mathbf{P} = (0, 0, P^z)$. In the case of longitudinal polarization, one has $\langle PS_z|J^z|PS_z\rangle = \hbar/2$ where S_z is spin polarization vector. The above equation is boost invariant along the z direction. This is a starting point to construct helicity (projection of the spin along the direction of motion) sum rules.

Using the gauge-invariant QCD AM in equation 5, the frame-independent sum rule[30,35] an be written as

$$\frac{1}{2}\Delta\Sigma(\mu) + L_q^z(\mu) + J_g(\mu) = \frac{\hbar}{2}, \tag{7}$$

where $\Delta\Sigma/2$ is the quark helicity contribution measured in the EMC experiment, and L_q^z is total quark OAM contribution including all flavours of quarks. Together, they give the total quark AM contribution J_q. The last term, J_g, is the gluon contribution. All contributions depend on the renormalization scheme and scale μ (which is different from the Lorentz index), which are usually taken to be dimensional regularization and (modified) minimal subtraction. It has been shown that both contributions are related to the form factors of the EMT, $J_{q,g} = [A_{q,g}(0) + B_{q,g}(0)]/2$ (REF.[30]).

The frame independence of the above sum rule means that the proton spin composition does not depend on its momentum as long as its helicity is well defined, be it in the finite-momentum frame or infinite-momentum frame. This is a nice feature because the wave function is clearly frame dependent.

Helicity sum rules can also be derived from the canonical expression of the QCD AM density in equation 4. Because of the gauge dependence, one might outright dismiss the physical relevance of such sum rules. However, as we shall explain in the next subsection, the gluon helicity contribution in the IMF is in fact physical. This prompts speculations that the quark and gluon canonical OAM might be measurable as well. Therefore, Robert Jaffe and Aneesh Manohar proposed a canonical spin sum rule in a nucleon state with $P^z = \infty$ (REF.[31])

$$\frac{1}{2}\Delta\Sigma(\mu) + \Delta G(\mu) + \ell_q(\mu) + \ell_g(\mu) = \frac{\hbar}{2}, \tag{8}$$

where ΔG is the gluon helicity and $\ell_{q,g}$ are the canonical quark and gluon OAM, respectively. There are numerous

Belinfante improvement procedure
A process leading to a symmetric and gauge-invariant energy-momentum tensor in gauge theories.

Boost invariant
A property that does not change under a boost Lorentz transformation.

Dimensional regularization
A process making momentum integrals finite at ultraviolet by changing the space-time dimensions.

(Modified) minimal subtraction
A process subtracting off-ultraviolet divergences in dimensional regularization, often leading to a resolution scale dependence μ.

studies on this sum rule in the literature because of its relevance to the parton physics of the proton. Precision studies of the renormalization scale μ dependence of $\Delta\Sigma$ and ΔG have been reported in REFS[36–38] (see also REFS[26,39] for the scale evolution of OAM contributions).

Other developments[40–43] have shown that the parton OAM can be closely connected to the quantum phase-space Wigner function or distribution[44,45]. As the Wigner function describes the quantum distribution of quarks and gluons in both spatial and momentum spaces, it is possible to construct the parton OAM by a properly weighted integral. This leads to an intuitive explanation of the OAM contributions in the above two sum rules. The difference between two OAMs, the so-called potential angular momentum, comes from two different ways to define gauge links in the Wigner functions[43], one of which can be interpreted as final-state interaction effects in scattering experiments[46,47].

There have been other attempts to use equation 4 to write sum rules in different frames and gauges, for example, the Coulomb gauge at finite hadron momentum[48]. However, these sum rules have no known experimental measurements and remain of pure theoretical interest[20,33]. Some of them are known to reduce to the Jaffe–Manohar sum rule in the IMF[49,50].

Why is the gluon helicity in bound states a physical quantity? In general, a gauge-dependent operator is not a physical observable and hence cannot be related to an experimental measurement. However, ΔG and OAM in IMF in equation 8 appears to be an exception. Why this is the case has been an interesting theoretical puzzle for many years, and has generated much debate in the literature[33,48,51–53]. The explanation is that the gauge symmetry has a simple meaning for 'on-shell' gluon partons.

Experimentally measurable ΔG is the first moment of the gauge-invariant polarized gluon distribution[54]

$$\Delta G(Q^2) = \int_0^1 dx\ \Delta g(x, Q^2),$$
$$\Delta g(x) = \frac{i}{2x(P^+)^2} \int \frac{d\lambda}{2\pi} e^{i\lambda x} \langle PS|F^{+\alpha}(0) W(0,\lambda n) \widetilde{F}_\alpha^{\ +}(\lambda n)|PS\rangle, \quad (9)$$

where $\widetilde{F}^{\alpha\beta} = \varepsilon^{\alpha\beta\mu\nu} F_{\mu\nu}/2$ (ε is a totally antisymmetric tensor with $\varepsilon^{0123} = 1$), and the light-front gauge link $W(0, \lambda n)$ is defined in the adjoint representation of SU(3), with $n^\mu = (1, 0, 0, -1)$ as a light-front vector and λ is the light-front distance. The light-front quantities have been rewritten in the standard notation $V^\pm = (V^0 \pm V^z)/\sqrt{2}$ after a Lorentz transformation. The total gluon helicity ΔG is clearly gauge invariant, but non-local. It does not seem to have a simple interpretation in a general gauge.

However, in the light-front gauge $A^+ = 0$, the non-local operator in equation 9 reduces to the gluon 'spin operator' in equation 4, and thus the experimental data on ΔG can be interpreted as the measurement of a contribution to the Jaffe–Manohar's spin sum rule in this particular gauge, suggesting that a gauge-variant operator might correspond to an experimental observable in a specific gauge. This suggestion has prompted much theoretical discussions about the meaning of gauge symmetry and numerous of experimentally unaccessible spin sum rules[20]. The fundamental reason for use of gauge-variant operators is, however, not about generalizing the concept of gauge invariance, but about the nature of the proton states in the IMF[49].

As realized by Carl Friedrich von Weizsäcker and Evan James Williams in electromagnetism[55,56], the gauge field strength in a fast-moving source is dominated by its transverse components. For a static charge, the electric field is purely longitudinal ($\mathbf{E} = \mathbf{E}_\parallel$ or without curl). As the charge moves with velocity v and define $\beta = v/c$, where c is the speed of light, the field lines start to contract in the transverse direction due to a Lorentz transformation. The moving charge forms an electric current that generates transverse magnetic fields

$$\mathbf{B} = \nabla \times \mathbf{A} = \nabla \times \mathbf{A}_\perp, \quad (10)$$

and the gauge potential $\mathbf{A}$ acquires a non-zero transverse component $\mathbf{A}_\perp$ (divergence free). At large β, the field strength is enhanced by a factor of $\beta\gamma$ ($\gamma = 1/\sqrt{1-\beta^2}$) in the transverse direction, whereas it is strongly suppressed in the longitudinal direction[55,56]. In the limit of $\beta \to 1$ (or $\gamma \to \infty$), $\mathbf{E}_\perp \approx \mathbf{B}$, and $|\mathbf{E}_\perp| \gg |\mathbf{E}_\parallel|$, so the electromagnetic field can be approximated as free radiation.

The radiation fields have only two physical degrees of freedoms, and the longitudinal one in the gauge potential is just a pure gauge. Thus, for an on-mass-shell photon, its helicity is physical and can be considered as gauge-invariant spin. It is possible to superimpose such on-mass-shell plane wave states with definite helicity to construct light modes with definite OAM, or so-called twisted light[57,58]. The gauge-invariant issue never arises because one always deals with physical polarization.

Analogously, the Weizsäcker–Williams approximation is also a valid picture for gluons in an ultrarelativistic proton[59]. In the IMF, the gluon can also be approximated as free radiation, thus it only has two physical transverse polarizations. $A^+ = 0$ is a physical gauge which leaves the transverse polarizations of the radiation field intact. This justifies $\mathbf{E} \times \mathbf{A} = \mathbf{E}_\perp \times \mathbf{A}_\perp$ as the physical gluon spin (helicity) operator in the Jaffe–Manohar sum rule. The above consideration also applies to the associated canonical OAM, ℓ_q^z and ℓ_g^z, which implies that there are partonic sum rules for them[60–62]. However, the associated canonical OAMs involve a transverse-momentum integral by construction and their scale evolutions are much more complicated[63,64].

The situation is quite different, however, if one considers colour fields inside a bound state that does not travel relativistically. The longitudinal gauge potential subjected to a gauge transformation then contains a physical component whose effects cannot be separated from the transverse part. The gluons become off-mass-shell and the longitudinal polarization does has physical significance. Only gauge-invariant operators can pick up the correct physics from the longitudinal part of the gluon potential.

On-shell
Physical particles with the correct energy-momentum relation are called on-shell or on-mass-shell; otherwise, they are called off-shell or off-mass-shell. Off-shell particles are virtual and can exist in interaction processes.

Light-front
The path or separation along a direction of a light cone.

Thus, it is the physical states in IMF that ensure the total gluon helicity is measured through $\mathbf{E}\times\mathbf{A}$. The spin operator can have any longitudinal pure gauge potential that does not contribute to the physical matrix elements. This situation is exactly opposite to the usual textbook formulation of gauge symmetry where the external states are gauge dependent and the operators must be gauge invariant. When transforming the IMF states into states with finite momentum through an infinite Lorentz transformation, $E_\perp \times A_\perp$ becomes a non-local operator in equation 9.

Sum rule for the transverse angular momentum. For transverse polarization along, for example, the x direction, the transverse AM operator J^x changes after the boost along z, and therefore, cannot be diagonalized simultaneously with P^z. However, its expectation value in a transversely polarized state is well defined[65]

$$\langle PS_x|J^x|PS_x\rangle = \gamma(\hbar/2), \tag{11}$$

where γ is the Lorentz boost factor. Therefore, the transverse AM J^x is a leading observable because it enhances under boost, a fact insufficiently appreciated in the literature. The potential contribution to the transverse AM from the non-intrinsic centre-of-mass motion has led to incorrect results in the literature[65–67].

If we define, $J_\perp^{q,g} = \langle PS_\perp|J_{\perp q,g}|PS_\perp\rangle/(\gamma S_\perp)$, then the quark and gluon contributions can again be related to the form factors in equation 6

$$J_\perp^{q,g} = (A_{q,g} + B_{q,g})/2, \tag{12}$$

$$J_\perp^q + J_\perp^g = \hbar/2. \tag{13}$$

Both equations are the same as those in the helicity case. However, the separation of the quark spin and orbital contributions are frame dependent, with the former contribution going to zero in the infinite-momentum limit[65].

A parton interpretation can be derived for the above result following an earlier suggestion in REFS[68,69]. The physical reason for the existence of a parton interpretation is that the transverse AM can be built from a longitudinal parton momentum with a transverse coordinate. One can define a partonic AM density[43,63,70]

$$\begin{aligned} J_\perp^q(x) &= x[q(x) + E_q(x)]/2, \\ J_\perp^g(x) &= x[g(x) + E_g(x)]/2, \end{aligned} \tag{14}$$

where $q(x)$ and $g(x)$ are the unpolarized quark/antiquark and gluon distributions, and $E_{q,g}(x)$ are a type of generalized parton distribution (GPD)[30]. GPDs are an extension of the well-known Feynman parton distribution and are defined as the off-diagonal matrix element between nucleon states with different momenta, similar to form factors. They depend on three kinematic variables: x the longitudinal momentum fraction for the parton, ξ the skewness parameter representing the momentum transfer between the nucleon states along the longitudinal direction, and $t = \Delta^2$ the momentum transfer Δ^μ squared. They can be systematically studied through a new class of exclusive hadronic reactions first discovered in REF.[30]. $J_\perp^{q,g}(x)$ are the AM densities carried by partons of momentum x in a transversely polarized nucleon in which partons are in general off the centre of mass[69]. Integrating $J_\perp^{q,g}(x)$ over x gives the total transverse AM carried by quarks and gluons, respectively.

Spin ab initio calculations in lattice QCD

As non-perturbative QCD is unusually difficult to solve directly, numerous models of the proton were proposed in the 1970s and 1980s, many of which use 'effective' degrees of freedom. An introduction to these models can be found in textbooks[7,8]. A newer one is the holographic model in which the proton is pictured as a quark and a diquark bound state[71]. As the connections between the model degrees of freedom and the fundamental ones are unknown, whereas high-energy experiments probe QCD quarks and gluons directly, we will discuss the theoretical calculations using QCD degrees of freedom only.

At present, the only systematic approach to solve the QCD proton structure is lattice field theory[72], in which quark and gluon fields are put on four-dimensional Euclidean lattices with finite spacing a, and the quantum correlation functions of fields are calculated using Feynman path integrals and Monte Carlo simulations. The physical limits are recovered when the lattice spacing a becomes sufficiently small compared with the physical correlation length, the lattice volume much larger than the hadron sizes and the quark masses close to the physical ones[73]. There are less systematic approaches, such as the Schwinger–Dyson (Bethe–Salpeter) equations[74] and instanton liquid models[75] in which a certain truncation is needed to find a solution. Although much progress has been made in these other directions, we focus on the lattice QCD method, which can be systematically improved.

A complete physical lattice calculation faces a number of obstacles. First, the total AM is a flavour-singlet quantity, and as such, one needs to compute the costly disconnected diagrams for the quarks. As up and down quarks are light and the physical propagators become singular in the massless limit, the required computational resources at the physical pion mass are very high. Moreover, gluon observables need be calculated to complete the picture, which are known to be very noisy and a large number of field configurations are needed for accuracy. At the same time, one needs to take the continuum and infinite volume limits into account. All of these add up to an extremely challenging computational task. However, a computation with all these issues taken into account has become feasible recently[76].

An additional challenge is present in quantities such as ΔG, usually defined in terms of light-front correlations with real-time dynamics. It is well-known that the real-time Monte Carlo simulations demand exponentially increasing resources. The developments in large-momentum effective theory (LaMET) have opened the door for the calculation of such time-dependent light-front correlations[77–79].

Flavour-singlet
A quantity defined by summing over all quark flavours.

Disconnected diagrams
Contributions in lattice quantum chromodynamics calculations, in which the quark operators do not connect with the external hadron states.

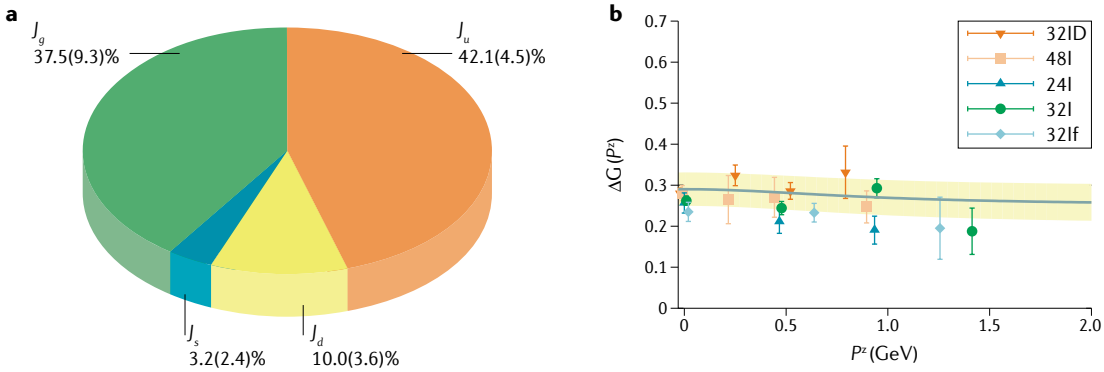

Fig. 1 | **State-of-the-art lattice quantum chromodynamics studies on the proton spin. a** | The spin decomposition in the frame-independent sum rule: the total spin contributions from the up (J_u), down (J_d), strange (J_s) quarks and gluons (J_g). The numbers come from the Extended Twisted Mass Collaboration[76] with 38.2(3.1)% from the total quark helicity contribution $\frac{1}{2}\Delta\Sigma$ and 18.8 (10.1)% from the total quark orbital angular L_q. **b** | The gluon spin is computed from different proton momenta along the z-direction (labelled as P^z on the horizontal axis) and lattice ensembles (denoted in the legend, see REF.[97] for details) by the χQCD collaboration[97]. The error bars represent the systematic and stastitcal uncertainties in this calculation. The yellow bands represent a fit of the lattice results using Eq. 15. The gluon spin reduces to the total gluon helicity ΔG contribution to Jaffe–Manohar sum rule when extrapolated to the infinite-momentum frame ($P^z \to \infty$): ΔG = 0.251(50) or 50(9)% of the proton spin, which can be compared to the Relativistic Heavy Ion Collider spin determination (FIG. 2). Part **b** adapted with permission from REF.[97], American Physical Society.

Frame-independent helicity sum rule. The matrix elements of local operators, $\Delta\Sigma$, J_q and J_g, are relatively easier to calculate using the standard lattice QCD technique. Much progress has been made in understanding the content of manifestly gauge-invariant helicity sum rule (and hence the transverse AM sum rule as well using equation 13).

The first calculation was performed for $\Delta\Sigma$ from different quark flavours[80]. The relevant studies in the last two decades have been summarized in a review[81]. Important progress has been made in chiral-fermion calculations[82] and at the physical quark mass[83]. The strange quark contribution has been calculated previously[84,85] with the anomalous Ward identity checked. The total quark spin contribution to the proton helicity has been consistently found to be about 40%.

The calculation of the total quark and gluon angular momenta started in REF.[86], where the quark part including the disconnected diagrams was calculated in the quenched approximation. The result of the total quark contribution is $J_q = 0.30 \pm 0.07$, that is 60%. Therefore, about 40% of the proton spin is carried by the gluons, through simple sum rule deduction. Following the quenched studies[87,88], dynamical simulations have now become a standard[89–93]. A first complete study of the AM decomposition was made in REF.[84], followed by a chiral dynamical simulation[94]. A first study at the physical quark mass appeared in REF.[83].

A high-precision dynamical simulation at the physical pion mass has been finished recently[76]. It was found that the total quark spin contribution is about 38.2%, and the orbital AM of the quarks about 18.8%, much reduced compared with the quenched simulations. The total gluon contribution is 37.5%. The resulting pie chart is shown in FIG. 1a. The total spin is 94.6% of $\hbar/2$ with an error bar of 14.2%. These results are largely consistent with the chiral fermion study in REF.[94]. All numbers are quoted in the minimal subtraction ($\overline{\text{MS}}$) scheme at $\mu = 2$ GeV.

Quenched approximation
A term referring to lattice quantum chromodynamics calculations in which the fermion determinant is neglected to save computational costs.

Gluon helicity in light-travelling protons. The calculation of the gluon helicity ΔG has not been possible for many years because it is defined from a time-dependent correlation function. However, in 2013, a breakthrough was finally made by studying the frame dependence of non-local matrix elements[49]. It was found that one can match the large-momentum matrix element of a static 'gluon spin' operator calculable in lattice QCD to ΔG in the IMF[49]. This idea was a prototype of LaMET, which was soon put forward as a general approach to calculate all parton physics[77,78].

The choice of the static 'gluon spin' operator is not unique. There is a universal class of operators[50] whose IMF limit approaches the free-field field operator in equation 4 in the light-front gauge. The simplest choice for the static 'gluon spin' is the free-field operator $\mathbf{E}\times\mathbf{A}$ fixed in a time-independent gauge. For example, the Coulomb gauge $\nabla\cdot\mathbf{A}=0$, or axial gauges $A^z=0$ and $A^0=0$ all maintain the transverse polarizations of the gluon field in the IMF limit, so they are viable options.

In the Coulomb gauge and $\overline{\text{MS}}$ scheme, the static 'gluon spin' $\Delta\widetilde{G}$ in a massive on-mass-shell quark state at one-loop order is[49,95]

$$\begin{aligned}\Delta\widetilde{G}(P^z,\mu)(2S^z) &= \langle PS|(\mathbf{E}\times\mathbf{A})^z|PS\rangle_q\big|_{\nabla\cdot\mathbf{A}=0} \\ &= \frac{\alpha_s C_F}{4\pi}\left[\frac{5}{3}\ln\frac{\mu^2}{m^2}-\frac{1}{9}+\frac{4}{3}\ln\frac{(2P^z)^2}{m^2}\right](2S^z),\end{aligned} \tag{15}$$

where $\alpha_s = g_s^2/4\pi$, $C_F = 4/3$ and the subscript q denotes a quark. The collinear divergence is regulated by the finite quark mass m. The above equation shows that the gluon state depends on the momentum P^z, as it should be. If we follow the procedure in REF.[96] and take $P^z \to \infty$ limit before ultraviolet regularization, which is the standard procedure to define partons[49], we obtain

$$\Delta G(\infty,\mu)(2S^z) = \langle PS|(\mathbf{E}\times\mathbf{A})^z|PS\rangle_q|_{\nabla\cdot\mathbf{A}=0} = \frac{\alpha_s C_F}{4\pi}\left(3\ln\frac{\mu^2}{m^2}+7\right)(2S^z), \quad (16)$$

which is exactly the same as the light-front gluon helicity $\Delta G(\mu)$ appearing in Jaffe–Manohar spin sum rule[51]. Therefore, despite the difference in the ultraviolet divergence, the infrared-sensitive collinear divergences of $\Delta\widetilde{G}(P^z,\mu)$ and $\Delta G(\mu)$ are exactly the same, which allows for a perturbative matching between them.

With the LaMET approach, ΔG was calculated in lattice QCD for the first time[97]. In this calculation, the static gluon spin operator $\mathbf{E}\times\mathbf{A}$ in the Coulomb gauge was simulated on the lattice and converted to the continuum $\overline{\text{MS}}$ scheme with one-loop lattice perturbation theory, which is shown in FIG. 1b. With leading-order matching and extrapolation to the IMF, the authors of REF.[97] obtained $\Delta G(\mu=\sqrt{10}\,\text{GeV}) = 0.251(47)(16)$, or 50(9)(3)% of the proton spin. A refined study on the systematics and precise matching should be made in the future.

Canonical OAM and transverse AM density in light-travelling proton. To complete the Jaffe–Manohar picture of the proton spin, one needs to compute the canonical OAM of the quarks and gluons in the IMF and light-front gauge. This can be done following the same approach outlined above for ΔG. A study of calculating these in LaMET has been made in REF.[98]. One can start from the matrix elements, for example, in Coulomb gauge and at finite momentum P^z

$$\widetilde{\ell}_q(\mu,P^z)(2S^z) = \left\langle PS\left|\int d^3\mathbf{x}\,\psi_f^\dagger(\mathbf{x}\times(-i\nabla))^z\psi_f\right|PS\right\rangle, \quad \widetilde{\ell}_g(\mu,P^z)(2S^z) = \left\langle PS\left|\int d^3\mathbf{x}\,E^{ia}(\mathbf{x}\times\nabla)^z A^{ia}\right|PS\right\rangle, \quad (17)$$

which can be matched onto $\ell_{q,g}(\mu)$ in the Jaffe–Manohar sum rule. The matching expressions have been worked out in the Coulomb gauge in REF.[99]. Mixings with potential AM contributions should also be taken into account[46]. As the matrix elements are spatial moments, one can either calculate them directly using $\mathbf{x}$ weighting on lattice[100,101], or by taking the zero-momentum-transfer limit of the momentum-density form factors. The computation of the canonical quark OAM from lattice QCD has been carried out in REFS[102,103] using non-local operators, for which matching to the IMF quantities has yet to be carried out.

A similar approach can be used to calculate the canonical OAM distributions $\ell_q(x,\mu)$ and $\ell_g(x,\mu)$ (REFS[60,62]). As both distributions are subleading in high-energy experiments (the so-called twist-three), they may contain a zero-mode contribution at $x=0$ (REFS[104,105]), which makes the experimental measurement of $\ell_{q,g}(\mu)$ through sum rules challenging. Mixings with other twist-three correlations with gluon fields must be considered.

Likewise, the transverse AM of the proton is a leading light-front observable, and has a partonic interpretation in terms of the transverse AM density $J_\perp^{q,g}(x) = x(\{q,g\}(x) + E_{q,g}(x))/2$. Although the singlet distributions $q(x)$ and $g(x)$ are well constrained and can be calculated on a lattice with the standard LaMET method[79], little is known about the GPDs $E_{q,g}(x)$. The moments of $E_{q,g}(x)$ can be calculated as a generalization of the form factors of the EMT. The x distributions can also be obtained directly as the spatial moment of the gauge-invariant momentum-density correlation functions.

Experimental progress and the EIC

We finally review the experimental progress in the search for the origins of the proton spin. Following the EMC, many experiments tried to confirm the result. First, we discuss efforts of nailing down the quark helicity contribution Δq, particularly Δs, from the semi-inclusive deep inelastic scattering (SIDIS), and the gluon helicity ΔG from polarized proton–proton collisions at the RHIC. Next, we review the measurement of the quark orbital AM contribution from a new class of experiments called deeply virtual Compton scattering, first proposed and studied in REFS[30,106]. Finally, we consider the prospects of studying the proton spin structure at the EIC.

Nailing down the quark and gluon helicities. The majority of experimental efforts followed the EMC experiment, measuring the polarized structure functions in DIS with polarized leptons on a polarized target (proton, neutron, deuteron). Two important initiatives have also emerged. First, the DIS experiment facilities extended their capabilities to measure the spin asymmetries in the semi-inclusive hadron production in DIS[107,108], helping to identify the flavour dependence in the polarized quark distributions. Second, the RHIC at the Brookhaven National Laboratory started the polarized proton–proton scattering experiments, which opened new opportunities to explore the proton spin, in particular, for the helicity contributions from gluon and sea quarks (virtual quark–antiquark pairs). Most of these efforts have been covered in the recent reviews[19,22].

The total quark spin contribution has been well determined from DIS measurements: $\Delta\Sigma \approx 0.30$ with uncertainties around 0.10, see, for instance, global analyses from REFS[109–111]. However, for sea quark polarizations including $\bar{u}$, $\bar{d}$ and s ($\bar{s}$), there exist larger uncertainties, in particular, in the strange quark polarization[110–112], where the constraints mainly come from SIDIS measurements by the HERMES and COMPASS experiments. It was also found that the W boson spin asymmetries at centre-of-mass energy $\sqrt{s} = 510\,\text{GeV}$ at the RHIC have also improved the constraints on the $\bar{u}$ and $\bar{d}$ polarization[113]. Exciting results, in particular, for the double spin asymmetries in inclusive jet production from the RHIC experiments have provided a stronger constraint on the gluon helicity[114] (FIG. 2). This constraint has great potential for future analyses from the RHIC experiments to further reduce the uncertainties owing to improved statistics[115,116]. However, due to the kinematic limitations, the total gluon helicity contribution still has a significant uncertainty.

Exclusive hard scattering
A hard scattering process in which specific final states with a fixed type of particle are produced.

Photon exclusive production
A hard scattering process in which only a photon is produced.

Bethe–Heitler amplitude
An elastic scattering amplitude in which only an extra photon is produced.

Quark OAM and GPD studies at JLab 12 GeV. It was found that the total quark (gluon) contribution to the proton spin (also the form factor of the QCD EMT) can be obtained from the moments of the GPDs[30]

$$J_q = \frac{1}{2}\Delta\Sigma_q + L_q = \lim_{t,\xi\to 0}\frac{1}{2}\int \mathrm{d}x\, x\,[H^q(x,\xi,t) + E^q(x,\xi,t)], \quad (18)$$

where H and E are GPDs, x is parton momentum fraction, ξ is the skewness and t is the momentum transfer squared. After subtracting the helicity contribution $\Delta\Sigma_q$ measured from the inclusive and semi-inclusive DIS experiments, the above equation will provide the quark OAM contribution to the proton spin. The GPDs can be measured in a new class of experiments called deep-exclusive processes, for example, deeply virtual Compton scattering (DVCS) and deeply virtual meson production (DVMP)[30,106,117,118]. Both DVCS and DVMP processes belong to exclusive hard scattering processes in lepton–nucleon collisions. For example, in the DVCS process, as shown in FIG. 3a, an incoming lepton scatters off the nucleon with momentum P and produces a high-momentum real photon, and the recoiling nucleon with momentum P'. In this way, the quark spatial position and momentum can be sampled simultaneously. Review articles for GPDs and DVCS can be found in REFS[119–122].

Experimental efforts using these processes have been made at various facilities, including HERMES at DESY[123], JLab 6 GeV (REF.[124]) and COMPASS at CERN[125].

In real photon-exclusive production, the DVCS amplitude interferes with the Bethe–Heitler amplitude. This will, on the one hand, complicate the analysis of the cross-section, and on the other hand, provide unique opportunities to directly access the DVCS amplitude through the interference. To obtain the constraints on the quark OAMs from these experiments, one needs to find the observables that are sensitive to the GPD Es. Experiments on the DVCS from JLab Hall A[124] and HERMES at DESY[123] have shown strong sensitivity to the quark OAMs in nucleon (see, for instance, FIG. 3b). In these experiments, the single spin asymmetries associated with beam or target in DVCS processes are measured, including the beam (lepton) single spin asymmetry and (target) nucleon single spin (transverse or longitudinal) asymmetries.

The JLab 12 GeV facility has just started its experimental programme. Multiple experiments on DVCS and DVMP are planned in the three experimental halls. A new generation of precision data for extracting quark GPDs is expected. From the phenomenology side, one needs to construct more sophisticated parametrizations for the GPDs. In particular, in light of the JLab experiments in next decade and future experiments at the EIC, a rigorous and collaborative approach has to be taken to perform the analysis of a large body of experimental data.

Prospects of the proton spin at the EIC. In early 2020, the US Department of Energy announced that the next major facility for nuclear physics in the United States will be a high-energy and high-luminosity polarized EIC

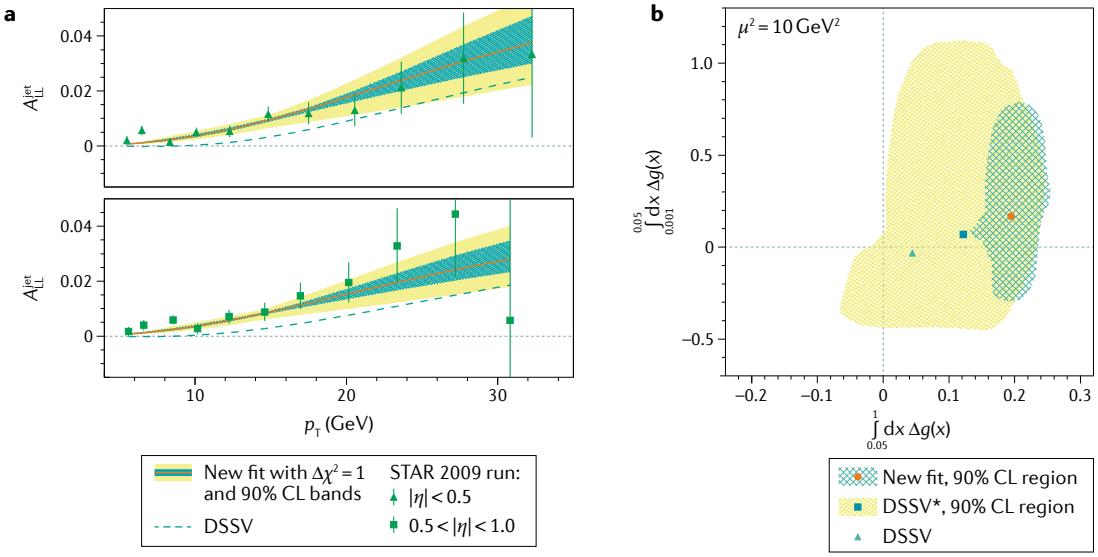

Fig. 2 | **The Relativistic Heavy Ion Collider at Brookhaven National Laboratory provides strong evidence for the gluon helicity contribution to the proton spin. a** | Double spin asymmetry A_{LL}^{jet} in inclusive jet production measured by the STAR collaboration[114], where LL stands for two proton beams both longitudinally polarized, as function of jet transverse-momentum p_T in GeV, compared with the global analysis (labelled as 'New fit') of de Florian–Sassot–Stratmann–Vogelsang (DSSV)[110], where the gluon helicity $\Delta g(x)$ is fitted. The data are displayed in small and medium rapidity η bins (upper and lower plots, respectively). χ^2 is the standard statistical test, and CL stands for confidence level. **b** | Constraints on the gluon helicity contribution to the proton spin from three fits (New fit, DSSV*, DSSV) to the experimental data at the resolution scale $\mu^2 = 10\,\mathrm{GeV}^2$, only the 'New fit' used the STAR data on the left. In the RHIC kinematics, that is, for $x > 0.05$, the integration over Δg was found to be positive and sizable: $\int_{0.05}^{1} \mathrm{d}x \Delta g(x) = 0.20^{+0.06}_{-0.07}$, as shown on the abscissa. The integral from the unexplored region of $x < 0.05$, shown on the ordinate, has large uncertainties. Parts **a** and **b** adapted with permission from REF.[110], American Physical Society.

to be built at the Brookhaven National Laboratory. The EIC will be the first polarized electron–proton collider and also the first electron–nucleus collider (FIG. 4a). The primary goal of the EIC is to precisely image gluon distributions in nucleons and nuclei, to reveal the origins of the nucleon mass and spin, and to explore the new QCD frontier of cold nuclear matter[23,24]. The EIC will impact our understanding of nucleon spin in many different ways. In the following, we highlight some of the most obvious ones:

- The quark and gluon helicity contributions to the proton spin are among the major emphases of the planned EIC. With the unique coverage in both parton momentum fraction x and resolution scale Q^2, it will provide the most stringent constraints on $\Delta\Sigma$ and ΔG (REF.[23]). FIGURE 4b shows the possible reduction in their uncertainties with the proposed EIC. Clearly, this will have a huge impact on our knowledge of these quantities, unparalleled by any other existing or anticipated facility.
- There will be a comprehensive research programme on gluon GPDs at the EIC. Apart from setting the first-hand constraints on the total quark/gluon AM contributions to the proton spin, the GPDs provide important information on the nucleon tomography, for example, the 3D imaging of partons inside the proton[45,68]. With wide kinematic coverage at the EIC, a particular example shown in FIG. 4c is that the transverse imaging of the gluon can be precisely mapped out from the detailed measurement of hard exclusive J/ψ production. Together with the gravitational form factors extracted from the DVCS, this will enable an unprecedented exploration of nucleon tomography and deepen our understanding of the nucleon spin structure. A pioneering experimental effort to constrain the gravitational form factor from DVCS at JLab has been carried out in REF.[126].
- The EIC may shed light on the quark/gluon canonical OAM directly through various hard diffractive processes. A particular example, studied in REFS[127,128], applies the connection between the parton Wigner distribution and the OAM[40–43] to show that the single longitudinal target-spin asymmetry in the hard diffractive dijet production is sensitive to the canonical gluon OAM distribution. The associated spin asymmetry leads to a characteristic azimuthal angular correlation between the proton momentum change and the relative transverse momentum between the quark–antiquark pair. With a special detector designed for the EIC, this observable can be well studied in the future, and will help obtain the final piece in the IMF helicity sum rule.

An important theoretical question concerns the asymptotic small-x behaviour of the polarized parton distribution functions and their contributions to the spin sum rule. There has been some progress to understand the proton spin structure at small x from the associated small-x evolution equations[129–134]. More theoretical efforts are needed to resolve the controversial issues that appeared in these derivations. The final answer to all these questions will provide important experimental guidelines for the future EIC, where proton spin structure is one of the major focuses.

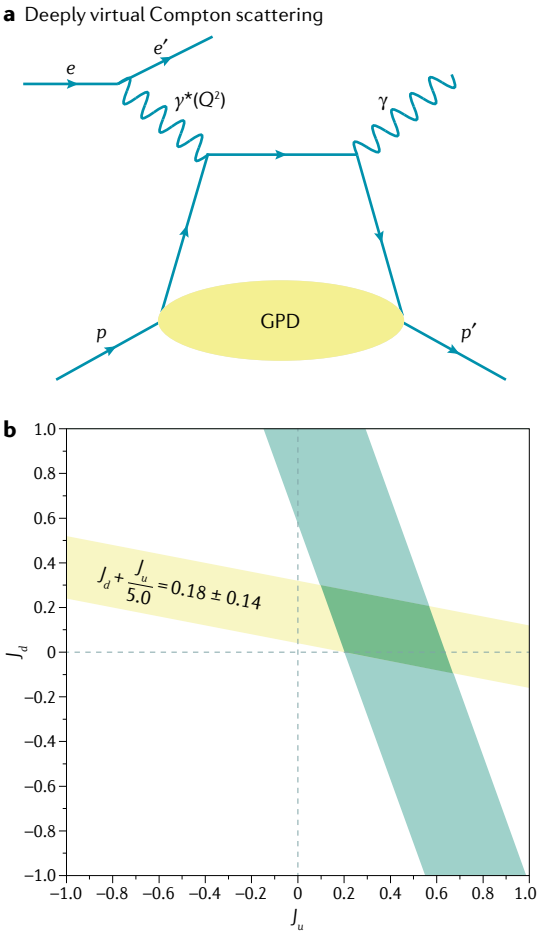

Fig. 3 | **Investigations of a new experimental process called deeply virtual Compton scattering, which has provided a way to study the quark orbital angular momentum in the proton. a** | A quark scattering mechanism for the deeply virtual Compton scattering (DVCS) process[106] where an electron (e) exchanges a virtual photon (γ^*) of invariant mass squared (Q^2) with the nucleon of momentum P, and produces a high-momentum real photon (γ) and a recoiling proton with momentum P'. DVCS probes the generalized parton distributions (GPDs), which describe the joint position and space information of the quarks and gluons. **b** | An example from the JLab Hall A (yellow, REF.[124]) and the HERMES data (green, REF.[135]) analysis of spin asymmetries in DVCS and the model-dependent constraints on the up and down quark total angular momentum, where a GPD model from REF.[136] was used in the analysis. J_u and J_d represent the spin contributions from the up and down quarks, respectively. Part **b** adapted with permission from REF.[124], American Physical Society.

Conclusion

More than 30 years after the EMC publication of the polarized DIS data, there has been much progress in understanding the spin structure. There are two well-established approaches to look at the composition of the proton spin: the frame-independent approach ('Ji sum rule') and the infinite-momentum-frame parton approach ('Jaffe–Manohar sum rule'). In the

Gravitational form factor
The energy-momentum form factor, derived from the fact that energy momentum is the charge for gravitational interaction.

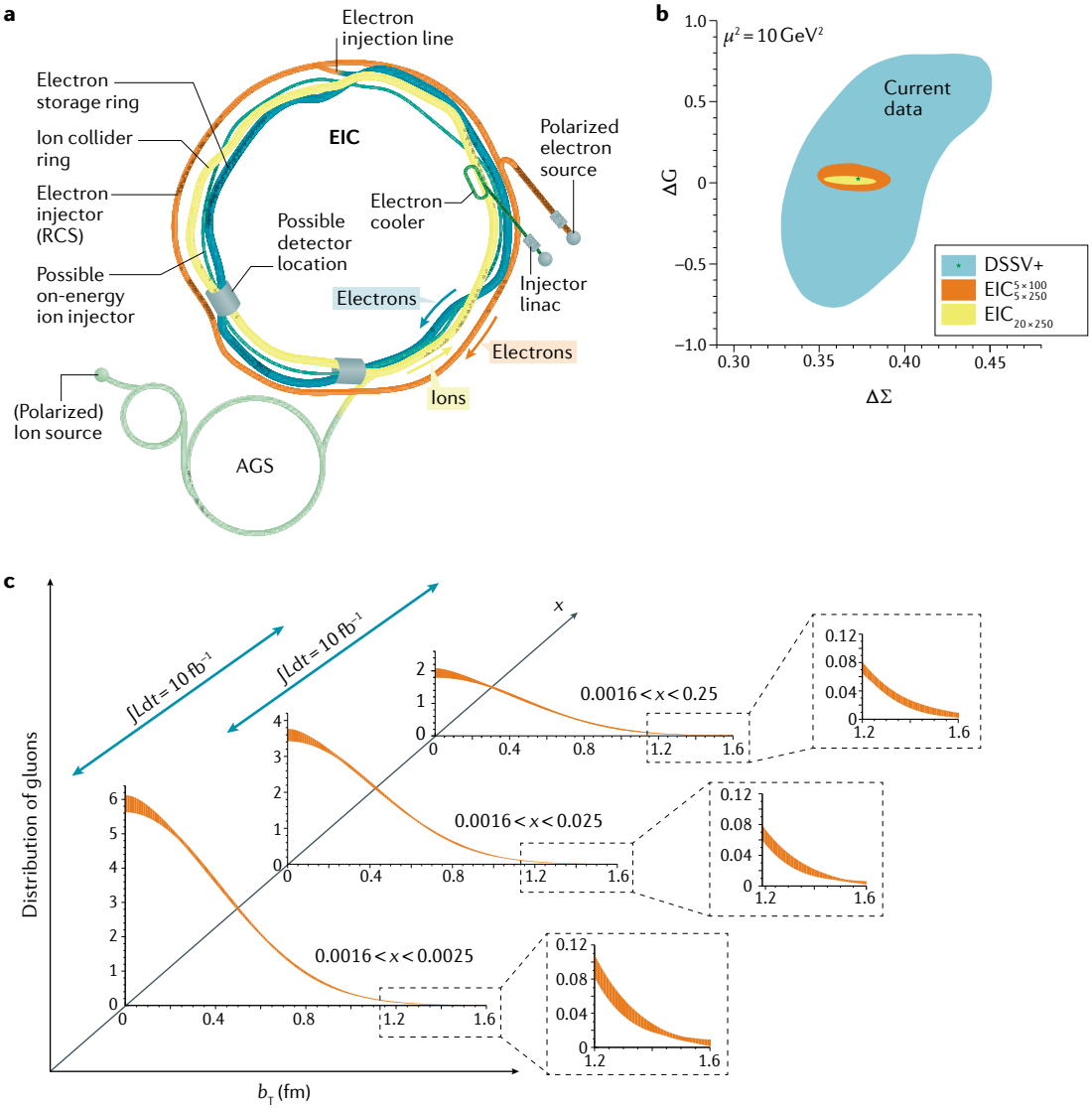

Fig. 4 | **The planned Electron-Ion Collider at Brookhaven National Laboratory and its expected impact on our understanding of nucleon spin. a** | Schematic of the experiment. AGS, alternating gradient synchrotron; RCS, rapid cycling synchrotron. **b** | The Electron-Ion Collider (EIC) precisions on the total quark helicity (ΔΣ) and gluon helicity (ΔG) contributions to the proton spin, calculated with different combinations of electron and proton energies (5 GeV on 100 GeV, 5 GeV on 250 GeV, 20 GeV on 250 GeV) at the resolution scale $\mu^2 = 10\,\mathrm{GeV}^2$. All uncertainties are calculated for $\Delta\chi^2 = 9$, where χ is the standard statistical test. The green star represents the central value of the global analysis of DSSV+ (stands for de Florian–Sassot–Stratmann–Vogelsang+, REF.[109]). **c** | The gluon distribution $g(x, b_T)$ in the transverse coordinate b_T for different gluon momentum fraction x from deeply virtual J/ψ-particle production at the EIC with photon invariant mass squared plus J/ψ-invariant mass squared 15.8–25.1 GeV^2, calculated with the integrated luminosity $\int Ldt = 10\,\mathrm{fb}^{-1}$ (fb, femtobarn). This process involves an electron (e)–proton (p) collision resulting in an electron, a proton and the state J/ψ, probing the generalized parton distribution for the gluon at small x. The Fourier transform with respect to the momentum transfer leads to the transverse spatial b_T distribution of gluons in the nucleon. High-precision measurements of this process at the EIC will provide a strong constraint on this tomography imaging. Panel **a** adapted with permission from the Brookhaven National Laboratory, 2020. Panels **b** and **c** adapted from REF.[23]., CC BY 4.0.

frame-independent approach, the quark orbital and gluon contributions can be obtained from the moments of the generalized parton distributions. Results from the JLab 6 GeV and HERMES data suggest a substantial quark orbital contribution. In the partonic picture of Jaffe and Manohar, the quark and gluon helicity have simple physics interpretation, and the result from the RHIC spin measurements has provided an important constraint on the total gluon helicity ΔG. The development of LaMET along with lattice QCD simulations provides the ab initio calculations of the spin structure, and the first results have provided an interesting overall picture. The JLab 12 GeV programme will provide better data on the quark GPDs and OAM. The EIC can provide high-precision measurements on the gluon helicity ΔG and total angular momentum contributions.

Published online 23 November 2020

1. Rutherford, E. Collision of α particles with light atoms. IV. An anomalous effect in nitrogen. *Phil. Mag. Ser. 6* **37**, 581–587 (1919).
2. Estermann, I., Frisch, R. & Stern, O. Magnetic moment of the proton. *Nature* **132**, 169–170 (1933).
3. Dirac, P. A. M. The quantum theory of the electron. *Proc. R. Soc. Lond.* **A117**, 610–624 (1928).
4. Skyrme, T. H. R. A unified field theory of mesons and baryons. *Nucl. Phys.* **31**, 556–569 (1962).
5. Gell-Mann, M. A schematic model of baryons and mesons. *Phys. Lett.* **8**, 214–215 (1964).
6. Zweig, G. *An SU(3) Model for Strong Interaction Symmetry and its Breaking* Version 1 Report CERN-TH-401 (CERN, 1964).
7. Bhaduri, R. K. *Models of the Nucleon: from Quarks to Solition* (Lecture Notes and Supplements in Physics Vol. 22, Addison-Wesley, 1988).
8. Thomas, A. W. & Weise, W. *The Structure of the Nucleon* (Wiley, 2001).
9. Fritzsch, H., Gell-Mann, M. & Leutwyler, H. Advantages of the color octet gluon picture. *Phys. Lett.* **47B**, 365–368 (1973).
10. Greenberg, O. W. Spin and unitary spin independence in a paraquark model of baryons and mesons. *Phys. Rev. Lett.* **13**, 598–602 (1964).
11. Isgur, N. & Karl, G. Positive parity excited baryons in a quark model with hyperfine interactions. *Phys. Rev. D* **19**, 2653–2677 (1979).
12. Close, F. E. *An Introduction to Quarks and Partons* (Academic Press, 1979).
13. Hughes, V. W. & Kuti, J. Internal spin structure of the nucleon. *Ann. Rev. Nucl. Part. Sci.* **33**, 611–644 (1983).
14. Ashman, J. et al. A measurement of the spin asymmetry and determination of the structure function g_1 in deep inelastic muon-proton scattering. *Phys. Lett. B* **206**, 340–346 (1988).
15. Ashman, J. et al. An investigation of the spin structure of the proton in deep inelastic scattering of polarized muons on polarized protons. *Nucl. Phys. B* **328**, 351–385 (1989).
16. Ellis, J. R. & Jaffe, R. L. A sum rule for deep inelastic electroproduction from polarized protons. *Phys. Rev. D* **9**, 1444-1446 (1974).
17. Filippone, B. W. & Ji, X.-D. The spin structure of the nucleon. *Adv. Nucl. Phys.* **26**, 1–88 (2001).
18. Bass, S. D. The spin structure of the proton. *Rev. Mod. Phys.* **77**, 1257–1302 (2005).
19. Aidala, C. A., Bass, S. D., Hasch, D. & Mallot, G. K. The spin structure of the nucleon. *Rev. Mod. Phys.* **85**, 655–691 (2013).
20. Leader, E. & Lorce, C. The angular momentum controversy: what's it all about and does it matter? *Phys. Rep.* **541**, 163–248 (2014).
21. Ji, X. Proton tomography through deeply virtual compton scattering. *Natl Sci. Rev.* **4**, 213–223 (2017).
22. Deur, A., Brodsky, S. J. & De Taramond, G. F. The spin structure of the nucleon. *Rep. Prog. Phys.* **82**, 076201 (2019).
23. Accardi, A. et al. Electron-Ion Collider: the next QCD frontier. *Eur. Phys. J. A* **52**, 268 (2016).
24. Boer, D. et al. Gluons and the quark sea at high energies: distributions, polarization, tomography. Preprint at http://arXiv.org/abs/1108.1713 (2011).
25. Tung, W. K. *Group Theory In Physics*, World Scientific Publishing Company (1985).
26. Ji, X.-D., Tang, J. & Hoodbhoy, P. The spin structure of the nucleon in the asymptotic limit. *Phys. Rev. Lett.* **76**, 740–743 (1996).
27. Ji, X. Comment on 'spin and orbital angular momentum in Gauge theories: nucleon spin structure and multipole radiation revisited'. *Phys. Rev. Lett.* **104**, 039101 (2010).
28. Bunce, G., Saito, N., Soffer, J. & Vogelsang, W. Prospects for spin physics at RHIC. *Ann. Rev. Nucl. Part. Sci.* **50**, 525–575 (2000).
29. Dudek, J. et al. Physics opportunities with the 12 GeV upgrade at Jefferson Lab. *Eur. Phys. J. A* **48**, 187 (2012).
30. Ji, X.-D. Gauge-invariant decomposition of nucleon spin. *Phys. Rev. Lett.* **78**, 610–613 (1997).
31. Jaffe, R. L. & Manohar, A. The g_1 problem: fact and fantasy on the spin of the proton. *Nucl. Phys. B* **337**, 509–546 (1990).
32. Noether, E. Invariant variation problems. *Gott. Nachr.* **1918**, 235–257 (1918).
33. Ji, X., Xu, Y. & Zhao, Y. Gluon spin, canonical momentum, and Gauge symmetry. *J. High Energy Phys.* **2012**, 82 (2012).
34. Belinfante, F. J. On the current and the density of the electric charge, the energy, the linear momentum and the angular momentum of arbitrary fields. *Physica* **7**, 449–474 (1940).
35. Ji, X.-D. Lorentz symmetry and the internal structure of the nucleon. *Phys. Rev. D* **58**, 056003 (1998).
36. Moch, S., Vermaseren, J. & Vogt, A. The three-loop splitting functions in QCD: the helicity-dependent case. *Nucl. Phys. B* **889**, 351–400 (2014).
37. Behring, A. et al. The polarized three-loop anomalous dimensions from on-shell massive operator matrix elements. *Nucl. Phys. B* **948**, 114753 (2019).
38. de Florian, D. & Vogelsang, W. Spin budget of the proton at NNLO and beyond. *Phys. Rev. D* **99**, 054001 (2019).
39. Thomas, A. W. Interplay of spin and orbital angular momentum in the proton. *Phys. Rev. Lett.* **101**, 102003 (2008).
40. Hatta, Y. Notes on the orbital angular momentum of quarks in the nucleon. *Phys. Lett. B* **708**, 186–190 (2012).
41. Lorce, C. & Pasquini, B. Quark Wigner distributions and orbital angular momentum. *Phys. Rev. D* **84**, 014015 (2011).
42. Lorce, C., Pasquini, B., Xiong, X. & Yuan, F. The quark orbital angular momentum from Wigner distributions and light-cone wave functions. *Phys. Rev. D* **85**, 114006 (2012).
43. Ji, X., Xiong, X. & Yuan, F. Proton spin structure from measurable parton distributions. *Phys. Rev. Lett.* **109**, 152005 (2012).
44. Ji, X.-D. Viewing the proton through 'color' filters. *Phys. Rev. Lett.* **91**, 062001 (2003).
45. Belitsky, A. V., Ji, X.-D. & Yuan, F. Quark imaging in the proton via quantum phase space distributions. *Phys. Rev. D* **69**, 074014 (2004).
46. Wakamatsu, M. More on the relation between the two physically inequivalent decompositions of the nucleon spin and momentum. *Phys. Rev. D* **85**, 114039 (2012).
47. Burkardt, M. Parton orbital angular momentum and final state interactions. *Phys. Rev. D* **88**, 014014 (2013).
48. Chen, X.-S., Lu, X.-F., Sun, W.-M., Wang, F. & Goldman, T. Spin and orbital angular momentum in gauge theories: nucleon spin structure and multipole radiation revisited. *Phys. Rev. Lett.* **100**, 232002 (2008).
49. Ji, X., Zhang, J.-H. & Zhao, Y. Physics of the gluon-helicity contribution to proton spin. *Phys. Rev. Lett.* **111**, 112002 (2013).
50. Hatta, Y., Ji, X. & Zhao, Y. Gluon helicity ΔG from a universality class of operators on a lattice. *Phys. Rev. D* **89**, 085030 (2014).
51. Hoodbhoy, P., Ji, X.-D. & Lu, W. Implications of color gauge symmetry for nucleon spin structure. *Phys. Rev. D* **59**, 074010 (1999).
52. Hoodbhoy, P. & Ji, X.-D. Does the gluon spin contribute in a gauge invariant way to nucleon spin? *Phys. Rev. D* **60**, 114042 (1999).
53. Hatta, Y. Gluon polarization in the nucleon demystified. *Phys. Rev. D* **84**, 041701 (2011).
54. Manohar, A. V. Polarized parton distribution functions. *Phys. Rev. Lett.* **66**, 289–292 (1991).
55. von Weizsacker, C. F. Radiation emitted in collisions of very fast electrons. *Z. Phys.* **88**, 612–625 (1934).
56. Williams, E. J. Correlation of certain collision problems with radiation theory. *Kong. Dan. Vid. Sel. Mat. Fys. Med.* **13N4**, 1–50 (1935).
57. Allen, L., Beijersbergen, M. W., Spreeuw, R. J. C. & Woerdman, J. P. Orbital angular momentum of light and the transformation of Laguerre–Gaussian laser modes. *Phys. Rev. A* **45**, 8185–8189 (1992).
58. Bliokh, K. Y. & Nori, F. Transverse and longitudinal angular momenta of light. *Phys. Rep.* **592**, 1–38 (2015).
59. Altarelli, G. & Parisi, G. Asymptotic freedom in parton language. *Nucl. Phys. B* **126**, 298–318 (1977).
60. Hagler, P. & Schafer, A. Evolution equations for higher moments of angular momentum distributions. *Phys. Lett. B* **430**, 179–185 (1998).
61. Harindranath, A. & Kundu, R. On orbital angular momentum in deep inelastic scattering. *Phys. Rev. D* **59**, 116013 (1999).
62. Bashinsky, S. & Jaffe, R. L. Quark and gluon orbital angular momentum and spin in hard processes. *Nucl. Phys. B* **536**, 303–317 (1998).
63. Hoodbhoy, P., Ji, X.-D. & Lu, W. Quark orbital-angular-momentum distribution in the nucleon. *Phys. Rev. D* **59**, 014013 (1999).
64. Hatta, Y. & Yao, X. QCD evolution of the orbital angular momentum of quarks and gluons: genuine twist-three part. *Phys. Lett. B* **798**, 134941 (2019).
65. Ji, X. & Yuan, F. Transverse spin sum rule of the proton, *Phys. Lett. B* **810**, 135786 (2020).
66. Bakker, B. L. G., Leader, E. & Trueman, T. L. A critique of the angular momentum sum rules and a new angular momentum sum rule. *Phys. Rev. D* **70**, 114001 (2004).
67. Leader, E. New relation between transverse angular momentum and generalized parton distributions. *Phys. Rev. D* **85**, 051501 (2012).
68. Burkardt, M. Impact parameter space interpretation for generalized parton distributions. *Int. J. Mod. Phys. A* **18**, 173–208 (2003).
69. Burkardt, M. Transverse deformation of parton distributions and transversity decomposition of angular momentum. *Phys. Rev. D* **72**, 094020 (2005).
70. Ji, X., Xiong, X. & Yuan, F. Transverse polarization of the nucleon in parton picture. *Phys. Lett. B* **717**, 214–218 (2012).
71. Brodsky, S. J., de Teramond, G. F., Dosch, H. G. & Erlich, J. Light-front holographic QCD and emerging confinement. *Phys. Rep.* **584**, 1–105 (2015).
72. Wilson, K. G. Confinement of quarks. *Phys. Rev. D* **10**, 2445–2459 (1974).
73. Rothe, H. J. Lattice gauge theories: an introduction. *World Sci. Lect. Notes Phys.* **43**, 1–381 (1992).
74. Maris, P. & Roberts, C. D. Dyson–Schwinger equations: a tool for hadron physics. *Int. J. Mod. Phys. E* **12**, 297–365 (2003).
75. Schafer, T. & Shuryak, E. V. Instantons in QCD. *Rev. Mod. Phys.* **70**, 323–426 (1998).
76. Alexandrou, C. et al. Complete flavor decomposition of the spin and momentum fraction of the proton using lattice QCD simulations at physical pion mass. *Phys. Rev. D* **101**, 094513 (2020).
77. Ji, X. Parton physics on a Euclidean lattice. *Phys. Rev. Lett.* **110**, 262002 (2013).
78. Ji, X. Parton physics from large-momentum effective field theory. *Sci. China Phys. Mech. Astron.* **57**, 1407–1412 (2014).
79. Ji, X., Liu, Y.-S., Liu, Y., Zhang, J.-H. & Zhao, Y. Large-momentum effective theory. Preprint at http://arXiv.org/abs/2004.03543 (2020).
80. Dong, S., Lagae, J.-F. & Liu, K. Flavor singlet g_A from lattice QCD. *Phys. Rev. Lett.* **75**, 2096–2099 (1995).
81. Lin, H.-W. et al. Parton distributions and lattice QCD calculations: a community white paper. *Prog. Part. Nucl. Phys.* **100**, 107–160 (2018).
82. Liang, J., Yang, Y.-B., Draper, T., Gong, M. & Liu, K.-F. Quark spins and anomalous ward identity. *Phys. Rev. D* **98**, 074505 (2018).
83. Alexandrou, C. et al. Nucleon spin and momentum decomposition using lattice QCD simulations. *Phys. Rev. Lett.* **119**, 142002 (2017).
84. Deka, M. et al. Lattice study of quark and glue momenta and angular momenta in the nucleon. *Phys. Rev. D* **91**, 014505 (2015).
85. Gong, M. et al. Strange and charm quark spins from the anomalous Ward identity. *Phys. Rev. D* **95**, 114509 (2017).
86. Mathur, N., Dong, S. J., Liu, K. F., Mankiewicz, L. & Mukhopadhyay, N. C. Quark orbital angular momentum from lattice QCD. *Phys. Rev. D* **62**, 114504 (2000).
87. Hagler, P. et al. Moments of nucleon generalized parton distributions in lattice QCD. *Phys. Rev. D* **68**, 034505 (2003).
88. Gockeler, M. et al. Generalized parton distributions from lattice QCD. *Phys. Rev. Lett.* **92**, 042002 (2004).
89. Brommel, D. et al. Moments of generalized parton distributions and quark angular momentum of the nucleon. *Proc. Sci.* **LATTICE2007**, 158 (2007).
90. Bratt, J. D. et al. Nucleon structure from mixed action calculations using $2+1$ flavors of asqtad sea and domain wall valence fermions. *Phys. Rev. D* **82**, 094502 (2010).
91. Syritsyn, S. N. et al. Quark contributions to nucleon momentum and spin from domain wall fermion calculations. *Proc. Sci.* **LATTICE2011**, 178 (2011).
92. Alexandrou, C. et al. Moments of nucleon generalized parton distributions from lattice QCD. *Phys. Rev. D* **83**, 114513 (2011).
93. Alexandrou, C. et al. Nucleon form factors and moments of generalized parton distributions using $N_f=2+1+1$ twisted mass fermions. *Phys. Rev. D* **88**, 014509 (2013).
94. Yang, Y.-B. A lattice story of proton spin. *Proc. Sci.* **LATTICE2018**, 017 (2019).
95. Chen, X.-S., Sun, W.-M., Wang, F. & Goldman, T. Proper identification of the gluon spin. *Phys. Lett. B* **700**, 21–24 (2011).

96. Weinberg, S. Dynamics at infinite momentum. *Phys. Rev.* **150**, 1313–1318 (1966).
97. Yang, Y.-B. et al. Glue spin and helicity in the proton from lattice QCD. *Phys. Rev. Lett.* **118**, 102001 (2017).
98. Zhao, Y., Liu, K.-F. & Yang, Y. Orbital angular momentum and generalized transverse momentum distribution. *Phys. Rev. D* **93**, 054006 (2016).
99. Ji, X., Zhang, J.-H. & Zhao, Y. Justifying the naive partonic sum rule for proton spin. *Phys. Lett. B* **743**, 180–183 (2015).
100. Gadiyak, V., Ji, X.-d. & Jung, C.-w. A lattice study of the magnetic moment and the spin structure of the nucleon. *Phys. Rev. D* **65**, 094510 (2002).
101. Blum, T. et al. Lattice calculation of hadronic light-by-light contribution to the muon anomalous magnetic moment. *Phys. Rev. D* **93**, 014503 (2016).
102. Engelhardt, M. Quark orbital dynamics in the proton from lattice QCD — from Ji to Jaffe–Manohar orbital angular momentum. *Phys. Rev. D* **95**, 094505 (2017).
103. Engelhardt, M. et al. From Ji to Jaffe–Manohar orbital angular momentum in lattice QCD using a direct derivative method. Preprint at http://arXiv.org/abs/2008.03660 (2020).
104. Aslan, F. & Burkardt, M. Singularities in twist-3 quark distributions. *Phys. Rev. D* **101**, 016010 (2020).
105. Ji, X. Fundamental properties of the proton in light-front zero modes, *Nuclear Physics B* **960**, 115181 (2020).
106. Ji, X.-D. Deeply virtual Compton scattering. *Phys. Rev. D* **55**, 7114–7125 (1997).
107. Airapetian, A. et al. Quark helicity distributions in the nucleon for up, down, and strange quarks from semi-inclusive deep-inelastic scattering. *Phys. Rev. D* **71**, 012003 (2005).
108. Alekseev, M. et al. Flavour separation of helicity distributions from deep inelastic muon-deuteron scattering. *Phys. Lett. B* **680**, 217–224 (2009).
109. de Florian, D., Sassot, R., Stratmann, M. & Vogelsang, W. Extraction of spin-dependent parton densities and their uncertainties. *Phys. Rev. D* **80**, 034030 (2009).
110. de Florian, D., Sassot, R., Stratmann, M. & Vogelsang, W. Evidence for polarization of gluons in the proton. *Phys. Rev. Lett.* **113**, 012001 (2014).
111. Nocera, E. R., Ball, R. D., Forte, S., Ridolfi, G. & Rojo, J. A first unbiased global determination of polarized PDFs and their uncertainties. *Nucl. Phys. B* **887**, 276–308 (2014).
112. Ethier, J. J., Sato, N. & Melnitchouk, W. First simultaneous extraction of spin-dependent parton distributions and fragmentation functions from a global QCD analysis. *Phys. Rev. Lett.* **119**, 132001 (2017).
113. Adam, J. et al. Measurement of the longitudinal spin asymmetries for weak boson production in proton-proton collisions at $\sqrt{s} = 510$ GeV. *Phys. Rev. D* **99**, 051102 (2019).
114. Adamczyk, L. et al. Precision measurement of the longitudinal double-spin asymmetry for inclusive jet production in polarized proton collisions at $\sqrt{s} = 200$ GeV. *Phys. Rev. Lett.* **115**, 092002 (2015).
115. Aschenauer, E.-C. et al. The RHIC SPIN program: achievements and future opportunities. Preprint at http://arXiv.org/abs/1501.01220 (2015).
116. Adam, J. et al. Longitudinal double-spin asymmetry for inclusive jet and dijet production in pp collisions at $\sqrt{s} = 510$ GeV. *Phys. Rev. D* **100**, 052005 (2019).
117. Collins, J. C., Frankfurt, L. & Strikman, M. Factorization for hard exclusive electroproduction of mesons in QCD. *Phys. Rev. D* **56**, 2982–3006 (1997).
118. Mankiewicz, L., Piller, G., Stein, E., Vanttinen, M. & Weigl, T. NLO corrections to deeply virtual Compton scattering. *Phys. Lett. B* **425**, 186–192 (1998).
119. Ji, X.-D. Off forward parton distributions. *J. Phys. G* **24**, 1181–1205 (1998).
120. Diehl, M. Generalized Parton Distributions. *Phys. Rep.* **388**, 41–277 (2003).
121. Ji, X. Generalized parton distributions. *Ann. Rev. Nucl. Part. Sci.* **54**, 413–450 (2004).
122. Belitsky, A. & Radyushkin, A. Unraveling hadron structure with generalized parton distributions. *Phys. Rep.* **418**, 1–387 (2005).
123. Airapetian, A. et al. Measurement of azimuthal asymmetries with respect to both beam charge and transverse target polarization in exclusive electroproduction of real photons. *J. High Energy Phys.* **2008**, 066 (2008).
124. Mazouz, M. et al. Deeply virtual Compton scattering off the neutron. *Phys. Rev. Lett.* **99**, 242501 (2007).
125. Akhunzyanov, R. et al. Transverse extension of partons in the proton probed in the sea-quark range by measuring the DVCS cross section. *Phys. Lett. B* **793**, 188–194 (2019).
126. Burkert, V., Elouadrhiri, L. & Girod, F. The pressure distribution inside the proton. *Nature* **557**, 396–399 (2018).
127. Ji, X., Yuan, F. & Zhao, Y. Hunting the gluon orbital angular momentum at the electron-ion collider. *Phys. Rev. Lett.* **118**, 192004 (2017).
128. Hatta, Y., Nakagawa, Y., Yuan, F., Zhao, Y. & Xiao, B. Gluon orbital angular momentum at small-x. *Phys. Rev. D* **95**, 114032 (2017).
129. Blumlein, J. & Vogt, A. The singlet contribution to the structure function $g_1(x,Q^2)$ at small x. *Phys. Lett. B* **386**, 350–358 (1996).
130. Kovchegov, Y. V., Pitonyak, D. & Sievert, M. D. Helicity evolution at small-x. *J. High Energy Phys.* **2016**, 72 (2016).
131. Kovchegov, Y. V., Pitonyak, D. & Sievert, M. D. Small-x asymptotics of the quark helicity distribution. *Phys. Rev. Lett.* **118**, 052001 (2017).
132. Kovchegov, Y. V. & Sievert, M. D. Small-x helicity evolution: an operator treatment. *Phys. Rev. D* **99**, 054032 (2019).
133. Boussarie, R., Hatta, Y. & Yuan, F. Proton spin structure at small-x. *Phys. Lett. B* **797**, 134817 (2019).
134. Tarasov, A. & Venugopalan, R. The role of the chiral anomaly in polarized deeply inelastic scattering I: finding the triangle graph inside the box diagram in Bjorken and Regge asymptotics. Preprint at http://arXiv.org/abs/2008.08104 (2020).
135. Ellinghaus, F., Nowak, W.-D., Vinnikov, A. & Ye, Z. Can the total angular momentum of u-quarks in the nucleon be accessed at HERMES? *Eur. Phys. J. C* **46**, 729–739 (2006).
136. Goeke, K., Polyakov, M. V. & Vanderhaeghen, M. Hard exclusive reactions and the structure of hadrons. *Prog. Part. Nucl. Phys.* **47**, 401–515 (2001).

Acknowledgements
This Review Article is dedicated to late V. Hughes whose drive in polarized DIS experiments lead to the surge and unabated interest in the proton spin structure, and perhaps to the EIC project in the United States. The authors thank C. Aidala, C. Alexandrou, M. Burkardt, Y. Hatta, D. Hertzog, R. Jaffe and K. F. Liu for useful communications relating to this article. This material is supported by the US Department of Energy, Office of Science, Office of Nuclear Physics, under contract numbers DE-AC02-05CH1123, DE-SC0012704 and DE-SC0020682, and within the framework of the TMD Topical Collaboration.

Author contributions
The authors contributed equally to all aspects of the article.

Competing interests
The authors declare no competing interests.

Peer review information
Nature Reviews Physics thanks Volker Burkert and the other, anonymous, reviewers for their contribution to the peer review of this work.